NOTICE CONCERNING COPYRIGHT RESTRICTIONS

Geothermal Exploration at Pilgrim Hot Springs, Alaska using Airborne Thermal Infrared Remote Sensing

Christian Haselwimmer[1], Anupma Prakash[1], and Gwen Holdmann[2]

[1]Geophysical Institute, University of Alaska Fairbanks
[2]Alaska Center for Energy and Power, University of Alaska Fairbanks
chha@gi.alaska.edu

Keywords

Pilgrim Hot Springs, Alaska, exploration, FLIR, thermal imaging, heat flux

ABSTRACT

The Department of Energy (DOE) and the Alaska Energy Authority are jointly funding a project to re-assess the resource potential of the Pilgrim Hot Springs geothermal system in western Alaska. Phase one of this project has included airborne thermal infrared remote sensing for mapping surface geothermal phenomena and assessment of the resource potential of the system. Thermal infrared and optical images were acquired over the Pilgrim Hot Springs site and neighboring regions during two surveys in fall 2010 and spring 2011. Thermal images providing information on land surface temperature at a spatial resolution better than 1.3 meters were acquired using a FLIR A320 camera operating in the broad 7.5−13 µm wavelength region. Fieldwork during the airborne surveys gathered ground calibration and validation data such as hot spring, ground, and atmospheric temperatures, atmospheric humidity and the precise GPS locations of low-emissivity ground targets. We applied atmospheric correction, registration and mosaicking to generate seamless maps of calibrated surface temperature across the study area. Analysis of this data enables delineation of the main geothermal features of the system including hot springs, pools, and areas of thermally anomalous ground. Using a thermal-budget approach the thermal heat flux sustaining surface geothermal waters was estimated from the fall and spring FLIR data. Calculated heat fluxes and outflow rates assuming a hot spring temperature of 81°C is significantly higher than previous field-based methods. Our work demonstrates that airborne thermal infrared remote sensing provides a rapid and relatively low cost method for mapping and quantitative assessment of undeveloped spring-dominated geothermal systems in Alaska.

1. Introduction

Access to reliable and relatively inexpensive sources of energy remains a significant issue for rural Alaskan towns and villages. Within the state, geothermal resources offer potential for providing one alternative to expensive fossil-fuel based energy but on the whole these resources remain poorly studied and exploited. Pilgrim Hot Springs on the Seward Peninsula, located approximately 75 km northeast of Nome (Figure 1), is a geothermal system that is currently being investigated as a potential energy source for Seward Peninsula communities. A project jointly funded by the Department of Energy (DOE) and the Alaska Energy Authority (AEA) is assessing the feasibility of developing Pilgrim Hot Springs as an active geothermal resource for power generation.

The initial phases of this project include undertaking a resource assessment as well as developing a conceptual model of the Pilgrim Hot Springs geothermal system. As part of this work we have used airborne thermal infrared remote sensing (Forward Looking Infrared Radiometer - FLIR) for the purposes of mapping the distribution and temperature of geothermal surface features associated with Pilgrim Hot Springs, to assess heat loss from these features as input into overall resource assessment, and as an exploration tool for mapping subtle thermal anomalies located away from the main springs site.

Airborne thermal infrared remote sensing has previously been applied with varying success to investigate geothermal hot springs in Alaska. Using high-altitude (60,000 feet) thermal images Dean et al. (1982) had limited success in differentiating warm ground and hot pools at Pilgrim Hot Springs that was due to the poor spatial and radiometric resolution of the thermal data. More recently, Dehn et al. (2006) used airborne thermal imagery to investigate surface geothermal pools at Chena Hot Springs, Alaska and found a close agreement between radiative heat loss estimates calculated from the thermal data and shallow conductive heat loss calculated using shallow temperature and well data. Elsewhere, airborne thermal images have been applied to map surface features and monitor the activity of the Yellowstone (Carr et al., 2009; Jaworowski et al., 2009) geothermal system in the USA and the Waimangu-Waiotapu (Mongillo, 1994) and Taupo (Hochstein and Dickinson, 1970) geothermal regions in New Zealand. In addition, thermal images have been used to directly quantify the heat flux from areas of geothermally heated ground (Bromley et al., 2011; Carr et al., 2009).

This paper presents an overview of the airborne thermal imaging work that we have undertaken as part of the Pilgrim Hot Springs project. The paper describes the methodology that we have used for the acquisition and processing of airborne thermal data to create calibrated mosaics of surface temperature and presents the results and our interpretations. The approach and results of calculating thermal flux associated with the hot springs/pools is also presented.

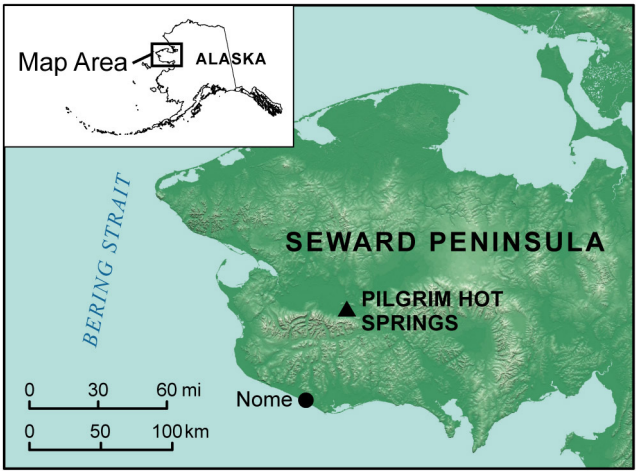

Figure 1. Location map of the study area.

2. Background

Pilgrim Hot Springs is located on the flood plain of the generally east-to-west meandering Pilgrim River. The site of the springs is marked by an approximately two square mile zone of thawed permafrost characterized by dense brush and cottonwoods that contrasts markedly with the surrounding stunted sub-arctic vegetation growing on unthawed, ~100m thick permafrost (Wescott and Turner, 1981). The geothermal system encompasses a shallow 90°C aquifer located between 15m and 35m below the surface, which is fed from deeper reservoirs of at least 150°C (Liss and Motyka, 1994). At the surface, hot water outflow occurs from a number of naturally occurring springs as well as from uncapped wells sunk into the geothermal aquifer. The rate of water discharge from the natural springs is estimated between 0.2 to 0.5 cfs with an energy content of 2 mw, given an average water temperature of 81°C (Harrison and Hawkins, 1980). In the regional context, Pilgrim Hot Springs is located on the downthrown block of a E-W trending graben system (Imuruk Basin) that is bound to south by the Kigluaik Fault and the up to 1200 meter elevation Kigluaik Mountains. The normal faulting and nearby basaltic volcanism led Turner and Swanson (1981) to propose a rift model for this part of the Seward Peninsula, which may provide the geothermal heat source via basic intrusions (Liss and Motyka, 1994). Although this provides a regional mechanism for the development of hot waters, no specific heat source or conduit has yet been identified for the Pilgrim Hot Springs geothermal system.

3. Methods

3.1. Airborne Data Acqusition

Thermal infrared and optical images were acquired over Pilgrim Hot Springs as part of two daytime airborne surveys flown with a fixed-wing aircraft during fall 2010 (10th September) and early spring (29th April) 2011 (Figure 2). The fall survey was flown at an altitude of 1000m and covered an ~200km^2 area centered on Pilgrim Hot Springs. This acquired data across a broad area with the aim of delineating geothermal features outside the main springs site that would provide targets for field investigation. The survey during the spring covered a smaller area (~10 km^2) focused on the main Pilgrim Hot Springs site and was flown at a lower altitude (750m) to acquire slightly higher spatial resolution thermal data. The spring timing of the most recent survey was selected to assess any seasonal variation in hot spring output as well as to investigate the effects of geothermally-heated ground on surface snow-melt. We used the results of the fall survey to inform the planning and geographic extents of the follow-up spring data acquisition.

Thermal images were acquired using a FLIR Systems A320 camera that records emitted thermal radiation in the 7.5 – 13 µm wavelength region using a 320 x 240, uncooled, microbolometer Focal Plane Array (FPA). The FLIR camera was fitted with an 18mm lens yielding pixel sizes of 1.3m and 1m, respectively for the 1000m and 750m flying heights. During the flight the FLIR was controlled with a laptop computer and the camera setup to record at 5 hz providing significant frame overlap in the along track direction. The flight lines were planned to ensure 30% sidelap thus providing complete coverage of the acquired thermal images for the survey areas. Along with the thermal data we acquired visible color imagery using a 12.1 megapixel Nikon D700 camera fitted with a calibrated 85mm lens that had been modified so that it was fixed at infinity. With this camera visible images with a pixel resolution of 15cm and 10cm, respectively were acquired at the two flying heights. We used a second laptop

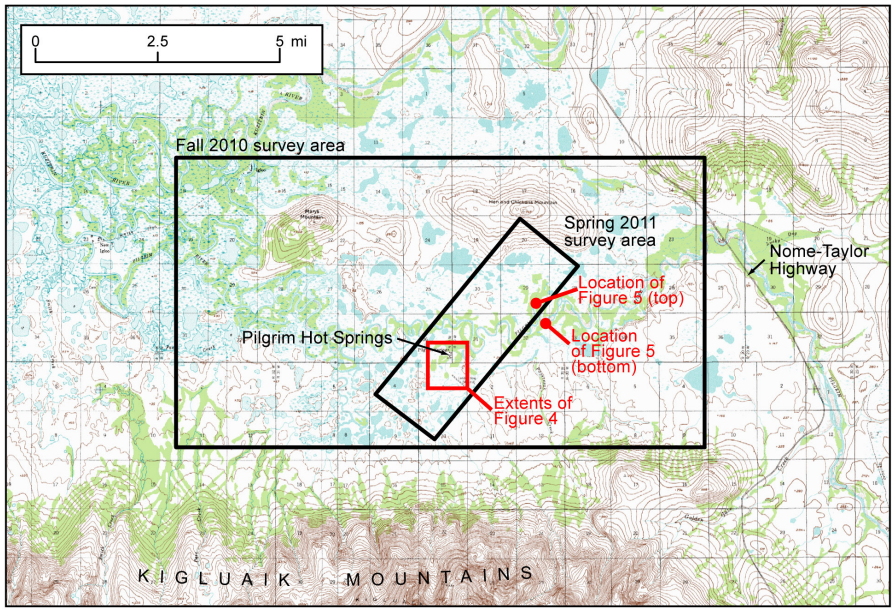

Figure 2. Extents of fall 2010 and spring 2011 airborne surveys over Pilgrim Hot Springs and locations of figures discussed in this paper.

computer and Topoflight Navigator software (http://www.topoflight.com/) to control the Nikon D700: the Topoflight software controlled the triggering of the camera at set intervals to achieve 30% along track coverage. Both the FLIR A320 and Nikon D700 cameras were mounted (with vibration dampening) in a nadir-looking orientation within the belly porthole of plane. We used a GPS/IMU system to continuously record accurate GPS position and exterior orientation parameters (i.e. plane roll, pitch and yaw) during the two flights.

During the periods of the airborne surveys various in-situ data were acquired as input into processing and calibration of the airborne data. We placed a number of space blankets throughout the study area to use as ground control points for registration of the thermal images: these present obvious cool points in the thermal imagery owing to the low emissivity of the aluminum foil space blankets. As input into atmospheric correction of the thermal data we recorded atmospheric temperature, humidity and wind speed using a hand-held instrument as well as data loggers (HOBO). The temperatures of different surface features (e.g. ground surface, snow, well-mixed hot pools) were recorded using temperature loggers and hand-held probes for the purposes of calibration and validation of the FLIR-derived surface temperature maps.

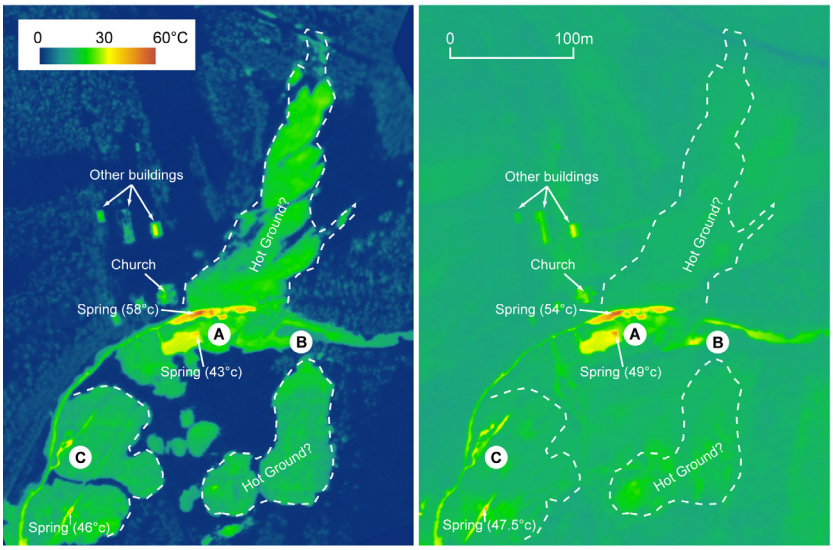

Figure 3. Mosaicked FLIR surface temperature maps for the northern part of Pilgrim Hot Springs (the area around the church) from the spring (left) and fall (right) airborne surveys. For the spring survey most of the area is snow-covered and colored in blue with the exception of areas of snow-melt (green) that may represent geothermally-heated ground (outlined with dotted lines). Circled letters refer to locations discussed in the text.

3.2 Image Processing

Initial processing of the airborne data involved manual registration of the Nikon D700 images. We are currently working on utilizing the exterior orientation information acquired during the flights to automate the registration and mosaicking of both the FLIR and D700 images. Manual registration of the D700 images was achieved by selecting common ground control points with a very high resolution (50cm pixel) WorldView 2 satellite image acquired over the study area.

Processing of the thermal images was applied to a subset of the 'most stable' frames: we selected a time interval necessary to achieve ~30% along track overlap and then selected the frame with the most stable roll value in each time period as queried from the IMU log. For the thermal image subset we calculated surface temperature values using the atmospheric correction procedure within the FLIR ThermaCam Researcher software. This was applied using the average flying height, atmospheric variables measured during the flight overpass and a fixed surface emissivity of 0.98. Each surface temperature image was then manually registered by selecting common points with the previously mosaicked D700 data. The registered frames were subsequently mosaicked to produce a seamless temperature map.

Comparison of the atmospherically corrected FLIR surface temperature data with in-situ temperature measurements (of hot pools, areas of snow, exposed ground) taken at the time of the flight overpass show that the airborne data consistently underestimates the surface temperature by 2 to 3°C. To correct these differences we calculated gain and offset values by plotting the average temperatures of homogeneous targets from the FLIR data against the corresponding in-situ temperature measurements for these features.

4. Mapping Surface Geothermal Features

The mosaicked surface temperature images acquired during the fall and spring surveys enable the clear delineation of geothermal surface features associated with Pilgrim Hot Springs (Figure 3). Geothermal waters and out-flowing springs are readily mapped by the relative contrast in temperature between these features and the surrounding land, surface streams/sloughs, and snow in the case of the spring survey data. Specific hot springs are observed as points displaying the highest relative temperature values mapped from the thermal imagery that form two broad groupings (Figure 4).

The hottest springs are located in a zone aligned roughly N-S that feed into the main curved slough/stream at the site (Figure 4). The temperature gradients within the stream suggest that hot spring waters flow both in a northerly and southerly direction and are the main source of water into this channel. Hot geothermal waters appear to cool to ambient temperature at some distance from the hot spring sources within this channel (marked by dashed lines on Figure 4). Around 350m west, another broadly N-S aligned zone of hot springs is observed. The water emanating from these sources is of lower temperature and feeds into a number of interconnected sloughs/ponds.

Comparison of the fall and spring data demonstrates that the temperature and location of hot springs as well as the extent of hot water is generally consistent between the two dates (Figure 3). This suggests that the production of hot water from the system is stable between fall and spring acquisitions. Having said this, there are some subtle differences in springs that may be observed between the two dates. For example, the hot springs around the main building complex at Pilgrim show some minor differences (see locations A, B, C on Figure 3): A) Two springs show variation in temperature and outflow from fall to spring; B) In the fall survey the spring at this location appears more active; C) There are some minor changes in the source of hot water between the fall and spring data at this location.

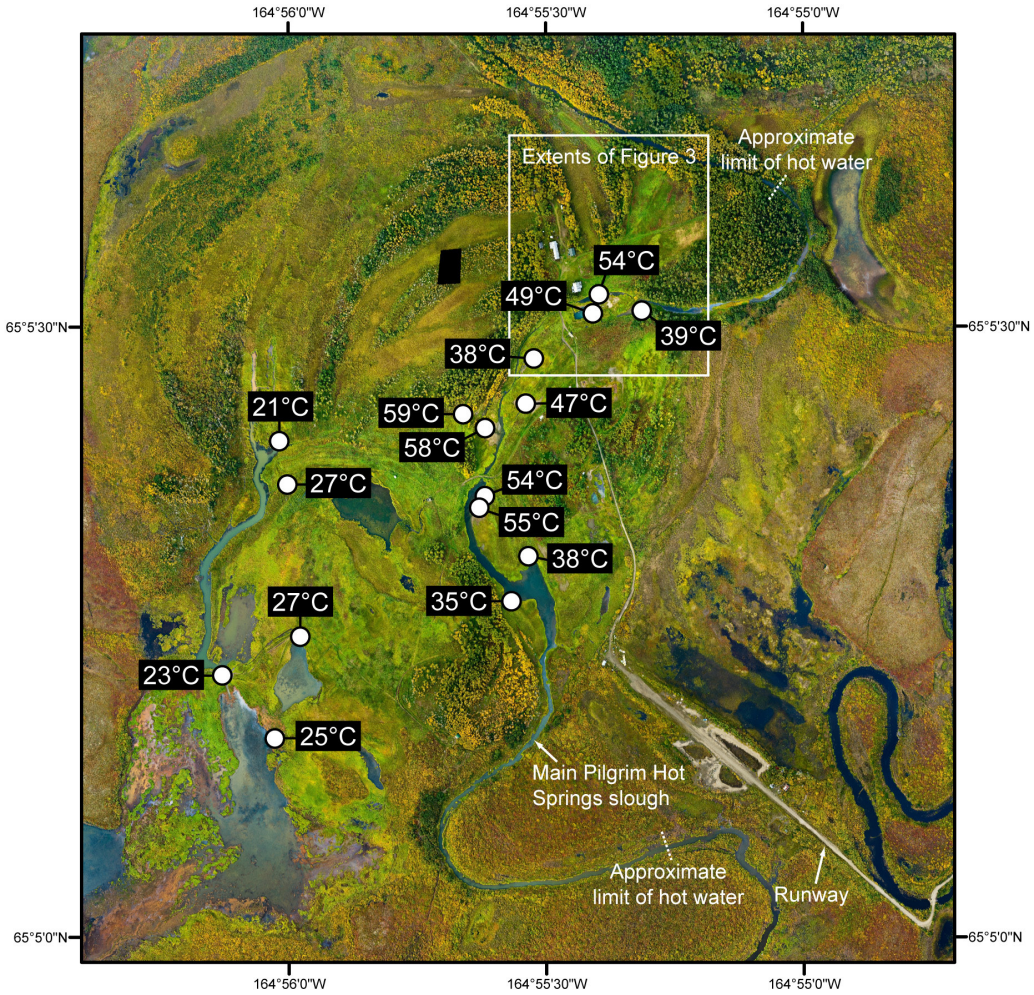

Figure 4. Map of hot spring locations and temperatures as determined from the FLIR surface temperature data acquired during the spring airborne survey. Dashed lines indicate the approximate locations at which geothermal waters cool to ambient temperature.

Comparison of hot spring temperatures derived from the FLIR data with published in-situ temperatures show some agreement but the analysis is restricted by the relatively few direct measurements (6 in total). For the two springs near the Church (location A, Figure 3), average in-situ measurements document a decline in hot spring temperature from 75.5°C to 35°C in the period from 1979 to 1993 (Liss and Motyka, 1994). Our FLIR-derived temperatures lie broadly in the middle of this range however, we consider that the thermal data probably underestimates true hot spring temperature for the following reasons: 1) the FLIR records the surface temperature of the hot pool, which may not be representative of the hot spring output temperature; 2) the FLIR records temperatures for pixels ~1m in size so there is a certain amount of averaging of true temperature values.

The combination of the fall and spring thermal data provides some evidence for geothermally-heated ground. Elevated land surface temperatures are evident from the fall data that may be related to geothermal heating. This interpretation is however, not exclusive as solar heating of exposed ground (soil or rock) may also be responsible for increased surface temperatures. The results of the spring survey highlight patches of anomalous snow melt that are consistent with some areas of elevated surface temperatures from the fall data (Figure 3). This supports the interpretation that these areas are in fact geothermally heated. At the time of the spring survey snow cover was continuous with the exception of melt patches around Pilgrim Hot Springs.

The thermal data from other parts of the survey areas (Figure 2) also indicate possible geothermal sources that provide targets for further field investigation (Figure 5). Around 3km northeast of Pilgrim Hot Springs, open water and elevated bank temperatures are observed along the Pilgrim River (Figure 5 top) in the spring survey data. At this time of year the Pilgrim River is frozen so the presence of open water is anomalous. The relationship between the exposed bank and the lack of river ice at this location may indicate outflow of heated geothermal waters. This would be consistent with previous workers interpretation of a second much smaller geothermal anomaly located in this area (Turner and Swanson, 1981). Further upstream of this feature (and around 1km southeast) a small stream is observed in the fall survey data that feeds into the main Pilgrim River (Figure 5 bottom). The waters in this stream are of higher temperature than the Pilgrim River and the source is poorly defined but broadly originating from the land immediately to the south. These observations may indicate spring activity fed by a geothermal source.

5. Estimating Heat Flux Associated with Surface Geothermal Waters

Using a thermal budget approach we calculated the heat flux sustaining surface geothermal waters as input into the overall resource assessment at Pilgrim Hot Springs. Although convective heat losses from the geothermal system are dominated by flow in the shallow aquifer, assessing the thermal flux and flow rate of the directly accessible surface geothermal waters provides a conservative baseline assessment of the resource potential. Heat losses associated with areas of geothermally heated ground are not discussed in this paper and will be the target for future research.

Our approach to using FLIR data to estimate the heat flux associated with surface geothermal waters (Haselwimmer et al., tion) has been adapted from previous work on calculating thermal losses from volcano crater lakes (Pasternack and Varekamp, 1997; Oppenheimer, 1996; Taran and Rouwet, 2008) and mud volcanos (Patrick et al., 2004). This approach is valid for Pilgrim Hot

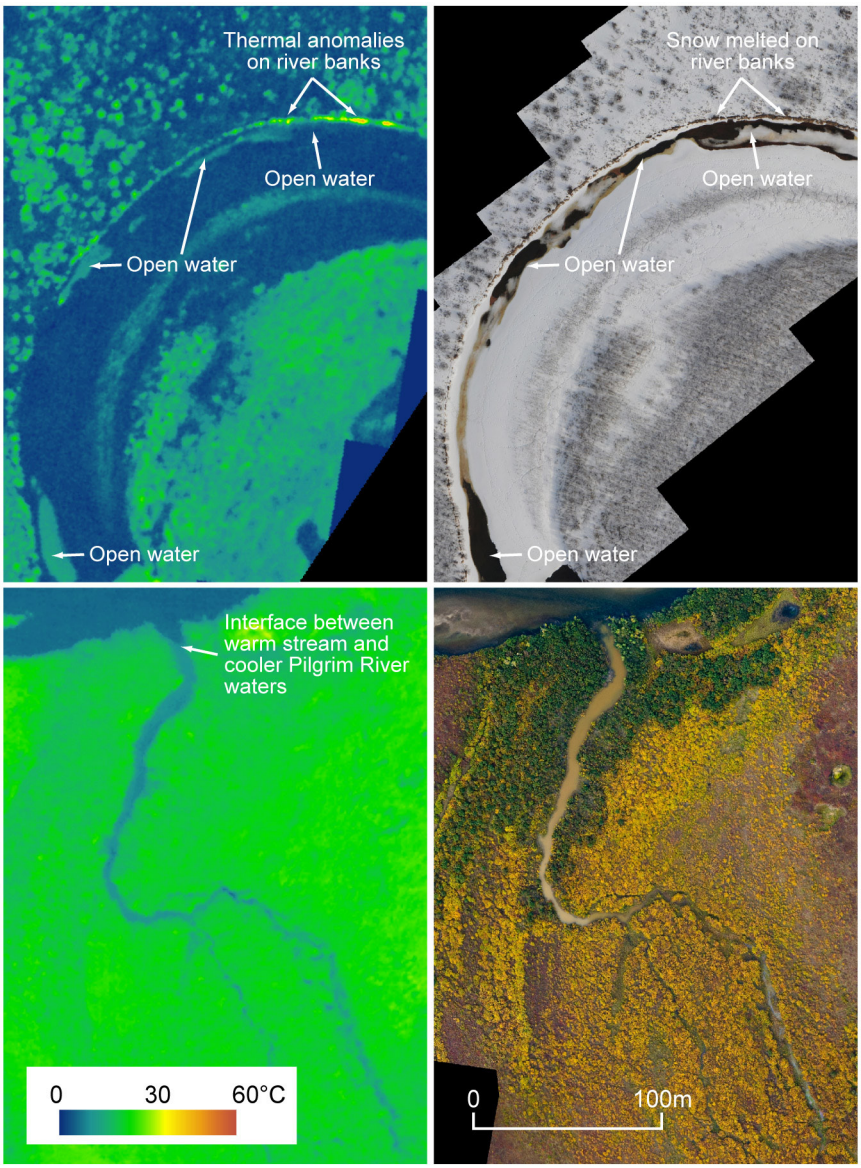

Figure 5. Examples of possible geothermal anomalies outside the main Pilgrim Hot Springs site. Top: FLIR (left) and optical (right) images of elevated surface temperatures and anomalous areas of open water along the banks of the Pilgrim River. Bottom: FLIR (left) and optical (right) images of a warm stream flowing into the Pilgrim River.

Springs as the main surface geothermal pool can be considered to be a closed system where there is limited heat transfer by advection out of the system (i.e. hot waters flowing into a river or lost via seepage). Following Oppenheimer (1996), the total heat budget for a body of water can be expressed by:

$$\Phi total = \Phi vol + \Phi ppt + \Phi seep + \Phi evap + \Phi sens + \Phi rad + \Phi sun + \Phi sky$$

where Φvol, Φppt, Φseep, Φevap, Φsens, Φrad, Φsun, Φsky are the energy fluxes (in Watts) associated with magmatic/hydrothermal inflow, precipitation, seepage, evaporation, conduction of sensible heat into the atmosphere, emitted radiation, incoming shortwave solar radiation, and incoming longwave radiation from the atmosphere, respectively. For this study we are interested in the Φvol term that represents the heat input from geothermal waters. There are several simplifications that we have made to this equation for the purposes of effectively calculating the geothermal flux. Heat inputs from precipitation (Φppt) and losses related to seepage (Φseep) are considered to be negligible when compared to the geothermal influx and so these terms are ignored. Secondly, we use the total heat flux for surface water at ambient temperature as an approximation of the incoming solar and atmospheric radiation. The rationale for this approach is that the temperature of non-geothermal surface waters (i.e. in ponds) will mainly represent solar and atmospheric heating.

This simplified heat budget model was implemented on a pixel-by-pixel basis by first delineating hot geothermal waters from the fall/spring FLIR temperature data using temperature thresholds. For each dataset we selected appropriate fixed values for the ambient temperature of water (16 and 8°C for the fall and spring data respectively). Geothermal heat flux ΦgeothermalP ixel was then calculated for each hot water pixel using:

$$\Phi geothermalPixel = (\Phi radP\ ixel + \Phi evapPixel + \Phi sensPixel) - (\Phi radAmbient + \Phi evapAmbient + \Phi sensAmbient)$$

where ΦradPixel, ΦevapPixel, and ΦsensPixel are the radiative, evaporative and sensible heat fluxes calculated at the temperature of the pixel, and ΦradAmbient, ΦevapAmbient, and ΦsensAmbient are the radiative, evaporative and sensible heat fluxes calculated at the ambient water temperature. Radiative heat fluxes were calculated with the Stefan-Boltzmann equation using a fixed emissivity of 0.98 that is appropriate for water. Evaporative and sensible heat fluxes were calculated using the formula of Ryan et al. (1974) that accounts for heat loss by free or forced convection. Inputs into this equation included the air temperature, atmospheric pressure and wind speed: for the fall and spring datasets we set the wind speed to 0.0 m/s as the output is particularly sensitive to this parameter and wanted to produce conservative modeled results for geothermal heat flux. For the geothermal heat flux estimates we calculated the corresponding outflow rates assuming a fixed hot spring temperature of 81°C (Harrison and Hawkins, 1980) using the specific enthalpy of water at the ambient and hot spring temperatures.

Our initial results of applying this method to the fall and spring FLIR data from Pilgrim Hot Springs yield heat flux estimates for the geothermal waters of 3.28 mw, and 3.80 mw respectively that correspond to outflow rates of 192.39 and 198.04 gpm. These estimates of hot spring heat flux are substantially higher than the ~2 mw figure that was previously calculated for Pilgrim Hot Springs (Harrison and Hawkins, 1980). The discrepancy is also likely to be higher as the FLIR-derived estimates are conservative: they do not take into account heat losses associated with seepage of hot water through the bed of hot pools, and we limited the component of forced convective heat loss by setting the wind speed

value to an unrealistic value of 0.0 m/s. The fact that there is a large difference between the FLIR-derived and existing directly measured values is consistent with the synoptic coverage of the thermal imagery (i.e. more hot springs can be mapped) and the difficulties with undertaking in-situ measurement of hot spring outflow particularly from undeveloped systems. Heat flux estimates between fall and spring are in generally good agreement and indicate that output from the system is stable over this period: the differences are consistent with variation in model parameters. We propose to validate the outcomes of this FLIR based method using in-situ measurements of spring temperature and outflow as well as using a chloride balance approach.

6. Discussion and Conclusions

In this paper we have presented an overview of our approach and results of airborne thermal infrared remote sensing during two surveys undertaken in the fall and spring over Pilgrim Hot Springs. The processed thermal data, providing mosaics of surface temperature, have been used to map the surface features associated with the geothermal system such as hot springs, pools and heated ground with unprecedented detail. This is the first time that a map of spring locations has been produced for the Pilgrim system and includes several sources not previously documented. Our comparison between the fall and spring survey data suggests that the temperature and rate of flow from the hot springs is generally consistent between the two dates. Observations of anomalous surface snow melt provide strong evidence for geothermaly-heated ground around the main Pilgrim Hot Springs site: these results provide potential targets for future shallow temperature surveys as well as deeper confirmation drilling. Some subtle indicators of possible geothermal sources were detected at distance from the main springs site that would be worthy of further field investigation.

The results of applying a simple thermal budget model to estimate the heat flux and outflow rates of hot spring waters has produced encouraging results that suggest surface geothermal waters account for up 3.8 mw of heat loss from Pilgrim Hot Springs. This figure is substantially higher than the ~2 mw previously suggested and the consistent nature of our new estimates between fall and spring imply a system with stable output.

7. Acknowledgements

This research is funded by the Department of Energy Geothermal Technologies Programme (CID: DE-EE0002846) and the Alaska Energy Authority Renewable Energy Fund Round III. We are extremely grateful to Jessie Cherry and Matt Nolan for their efforts on airborne system integration as well as data acquisition. We would also like to thank Markus Mager, Forrest Kirst, Peter Illig, Kate Schaefer and Jonathan O'Toole for their work during the airborne surveys.

References

Bromley, C., van Manen, S., and Mannington, W. (2011). Heat flux from steaming ground: reducing uncertainties. In *Thirty-Sixth Workshop on Geothermal Reservoir Engineering*, Stanford University, Stanford, California.

Carr, B., Heasler, H., and Jaworowski, C. (2009). Airborne reconnaissance of hydrothermal areas using daytime thermal infrared imagery.

Dean, K. G., Forbes, R. B., Turner, D. L., Eaton, F. D., and Sullivan, K. D. (1982). Radar and infrared remote sensing of geothermal features at Pilgrim Springs, Alaska. *Remote Sensing of Environment*, 12(5):391–405.

Dehn, J., Prakash, A., and Dean, K. (2006). Unpublished final FLIR report for Chena Hot Springs resort. Technical report.

Harrison, W. and Hawkins, D. (1980). Water and heat flow measurements and their relationship to power estimates at Pilgrim Springs, Alaska. Technical report, University of Alaska, Geophysical Institute.

Haselwimmer, C., Prakash, A., and Holdmann, G. (in preparation.). Estimating heat flux and flow rates of surface geothermal waters at Pilgrim Hot Springs, Alaska from airborne thermal imagery.

Hochstein, M. P. and Dickinson, D. J. (1970). Infra-red remote sensing of thermal ground in the Taupo Region, New Zealand. *Geothermics*, 2(Part 1):420, IN7–IN8, 421–423.

Jaworowski, C., Heasler, H., Neale, C., Cardenas, B., and Sivarajan, S. (2009). Using night-time, thermal infrared, imagery to remotely monitor the hydrothermal system at Hot Spring Basin, Yellowstone National Park.

Liss, S. and Motyka, R. (1994). Pilgrim Springs KGRA, Seward Peninsula, Alaska: Assessment of fluid geochemistry. *Geothermal Resources Council Transactions*, 18.

Mongillo, M. (1994). Aerial thermal infrared mapping of the Waimangu-Waiotapu Geothermal Region, New Zealand. *Geothermics*, 23(5/6):511–526.

Oppenheimer, C. (1996). Crater Lake heat losses estimated by remote sensing. *Geophys. Res. Lett.*, 23(14):1793–1796.

Pasternack, G. B. and Varekamp, J. C. (1997). Volcanic lake systematics i. physical constraints. *Bulletin of Volcanology*, 58(7):528–538.

Patrick, M., Dean, K., and Dehn, J. (2004). Active mud volcanism observed with landsat 7 etm+. *Journal of Volcanology and Geothermal Research*, 131(3-4):307–320.

Ryan, P. J., Harleman, D. R. F., and Stolzenbach, K. D. (1974). Surface heat loss from cooling ponds. *Water Resour. Res.*, 10(5):930–938.

Taran, Y. and Rouwet, D. (2008). Estimating thermal inflow to El Chichón crater lake using the energy-budget, chemical and isotope balance approaches. *Journal of Volcanology and Geothermal Research*, 175(4):472–481.

Turner, D. and Swanson, S. (1981). Continental rifting -a new tectonic model for the Central Seward Peninsula. Technical Report UAG R-284, University of Alaska, Geophysical Institute.

Wescott, E. and Turner, D. (1981). Geothermal reconnaissance survey of the Central Seward Peninsula. Technical report.